Electronic Supplementary Material (ESI) for Dalton Transactions.

Supplementary Information

Reduction-Induced Carbon Monoxide Dissociation by a $[Mn(bpy)(CO)_4][SbF_6]$ Complex and the Relevance in Electrocatalytic CO_2 Reduction

Hsin-Ya Kuo, Steven E. Tignor, Tia S. Lee, Danrui Ni, James Eujin Park, Gregory D. Scholes, and Andrew B. Bocarsly*

Department of Chemistry, Princeton University, Princeton, New Jersey 08544, United States

*Email: bocarsly@princeton.edu

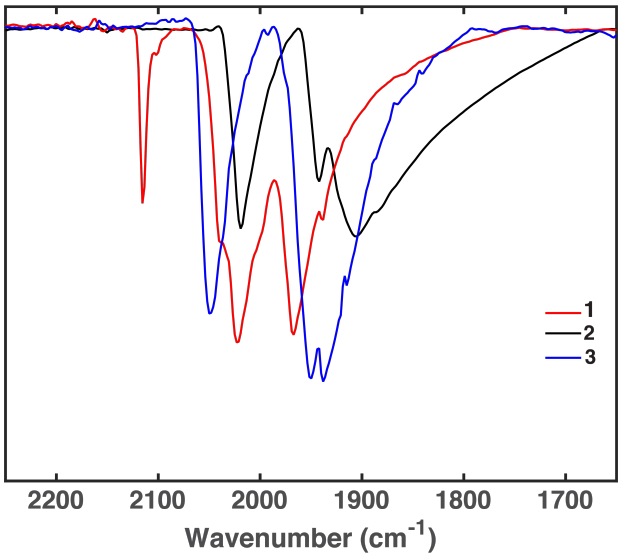

Figure S1 ATR-IR spectra of $[Mn(bpy)(CO)_4][SbF_6]$ (**1**), $[Mn(bpy)(CO)_3Br]$ (**2**) and $[Mn(bpy)(CO)_3(MeCN)][PF_6]$ (**3**).

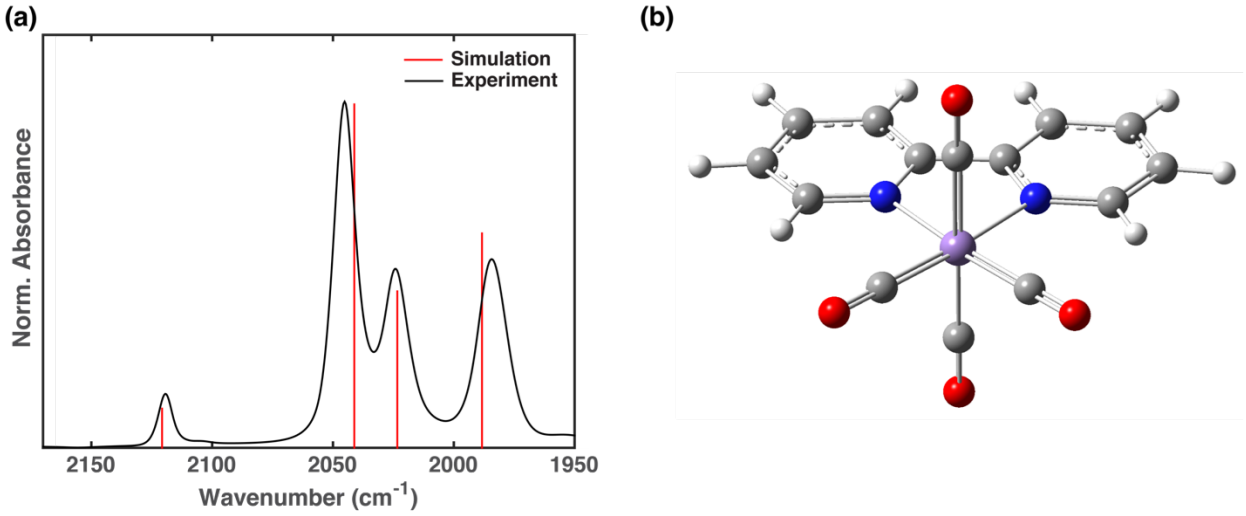

Figure S2 (a) DFT-calculated and experimental vibrational spectra of **1**. A scaling factor of 0.963 was determined by a comparison of the calculated and experimental data. (b) An optimized structure of **1** at the M06 level of theory.

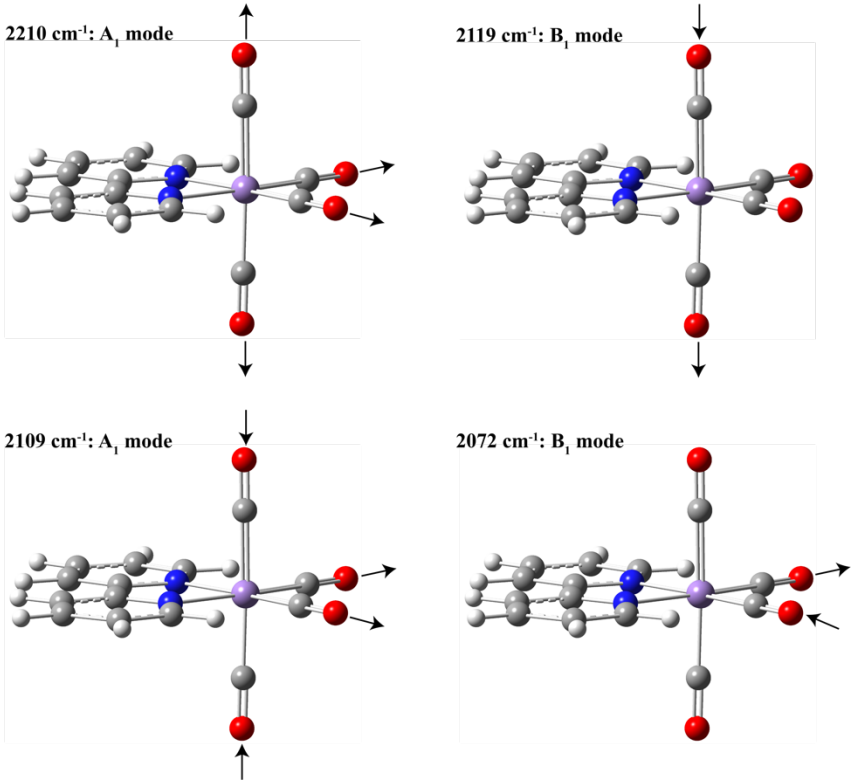

Figure S3 Displacement vectors for the carbonyl stretching modes of **1** (the vibrational frequencies are unscaled).

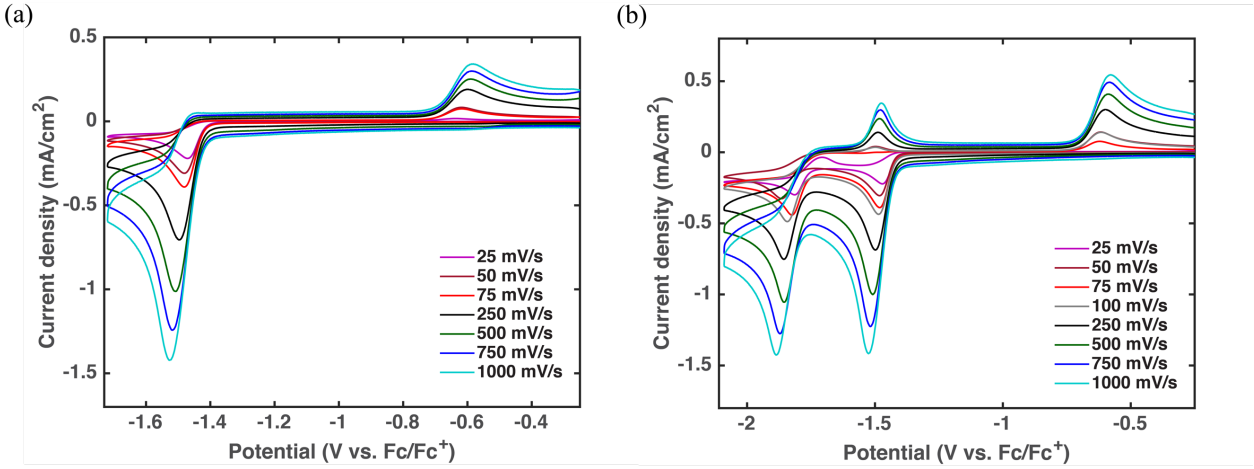

Figure S4 CV data of **1** (1 mM) under Ar in 0.1 M TBAH in MeCN. The switching potential was set to -1.70 V vs Fc/Fc^+ (a) and -2.10 V vs Fc/Fc^+ (b).

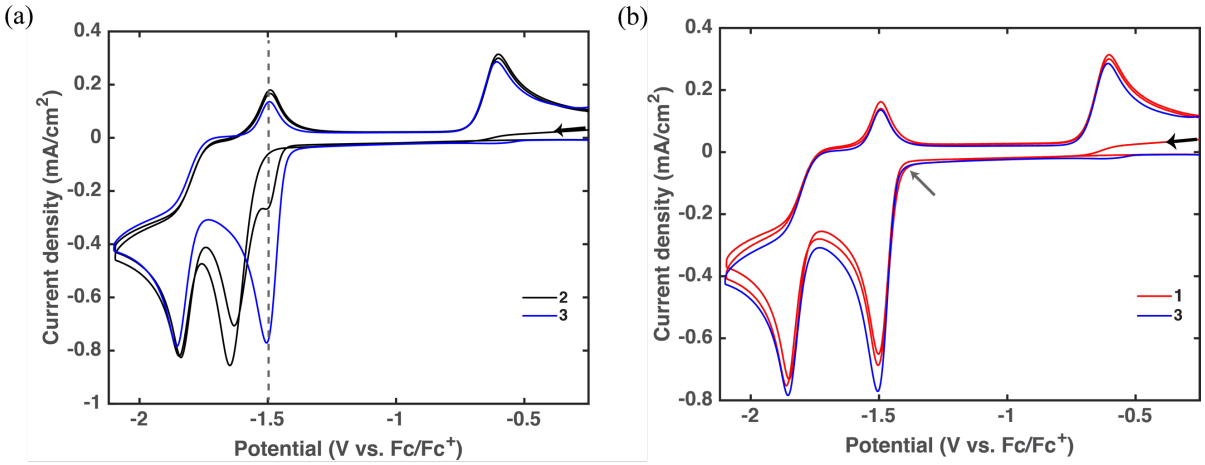

Figure S5 CV overlay of **2** and **3** (a) and **1** and **3** (b) at 250 mV/s under Ar. At the second scan (indicated by the black arrow), complex **1** exhibits the reductive current initializing at the different potential (grey arrow), and complex **2** shows the additional shoulder peak (as indicated by the dashed line).

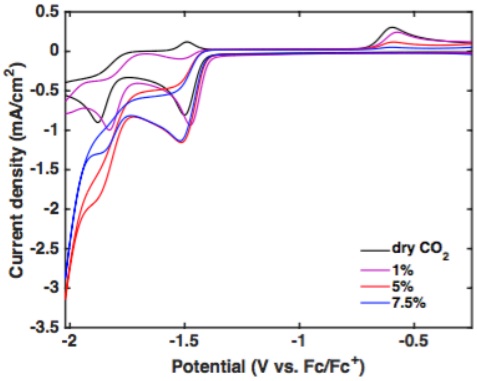

Figure S6 CV data of **1** with increasing amounts of H_2O added under CO_2 at 250 mV/s.

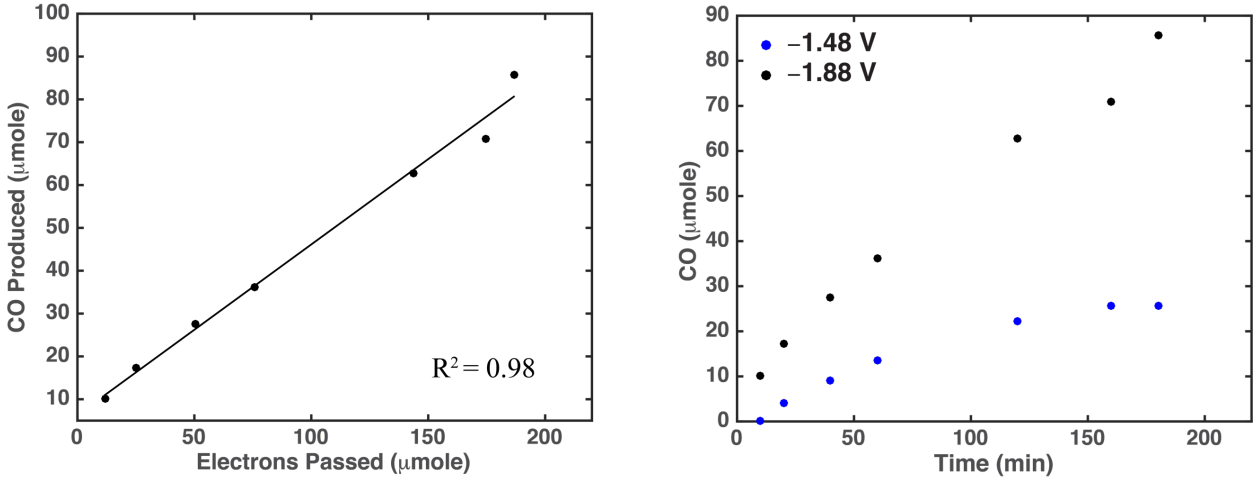

Figure S7 (a) CO production versus the moles of electrons consumed (two electrons per CO molecule). The slope represents an 80 ± 4.0% FE for the conversion of CO_2 to CO. Data were collected at -1.88 V vs Fc/Fc^+ with **1** (1 mM) loaded in CO_2-saturated 0.1 M TBAH in MeCN with 5% H_2O. (b) Comparison of CO detected at the first and second reduction potentials. All the other conditions were similar to those given in panel a.

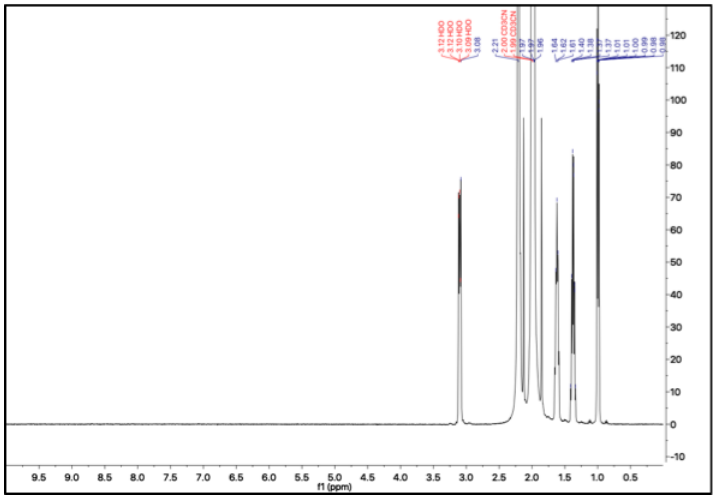

Figure S8 A sample ^1H NMR spectrum in CD_3CN of the worked-up 3 h bulk electrolysis of **1** (1 mM). No formate signal was observed at 8.5 ppm.

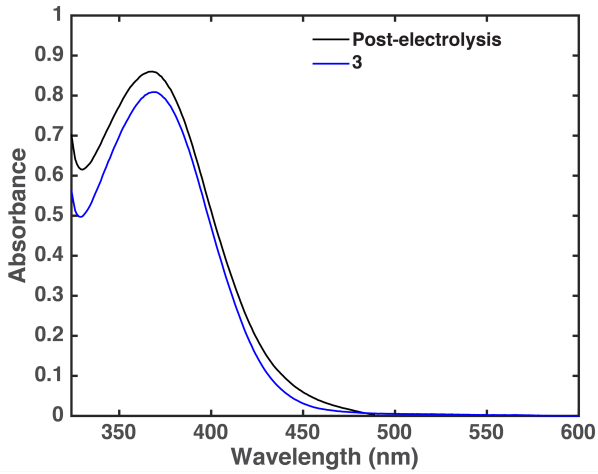

Figure S9 . UV-Vis spectra of a sample (1:4 dilution) after a 3 h bulk electrolysis at -1.48 V vs Fc/Fc^{+} with complex **1** (200 μM) in 0.1 M TBAH in MeCN. This result supports that after a single-electron reduction, complex **1** undergoes CO dissociation followed by solvolysis. The molarity of the resulting species in the electrolyte corresponds to 0.9 mM complex **3** (e = 4,246 $dm^3\ mol^{-1}\ cm^{-1}$).

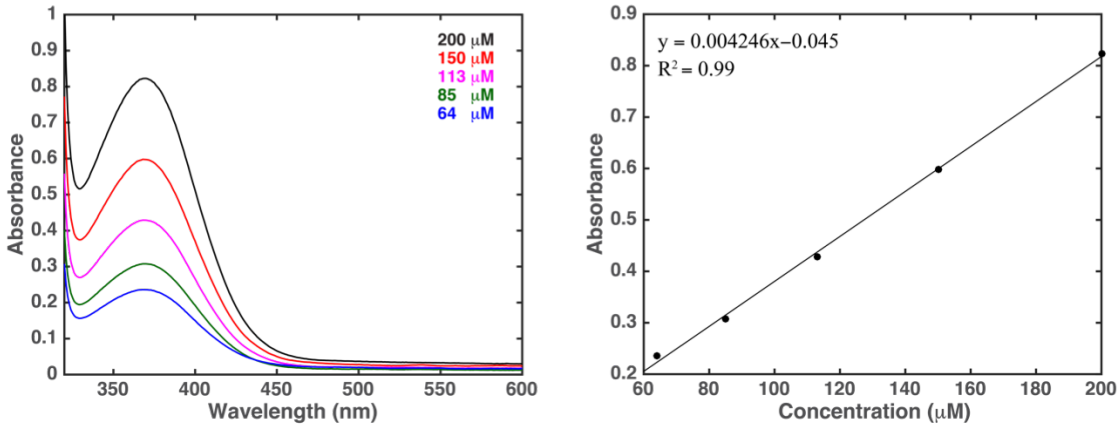

Figure S10 UV-Vis spectra of **3** in 0.1 M TBAH in MeCN at varied concentrations (left) and absorption at 370 nm as a function of the concentration (right). The molar absorptivity of **3** obtained from the slope is 4,246 $dm^3\ mol^{-1}\ cm^{-1}$.

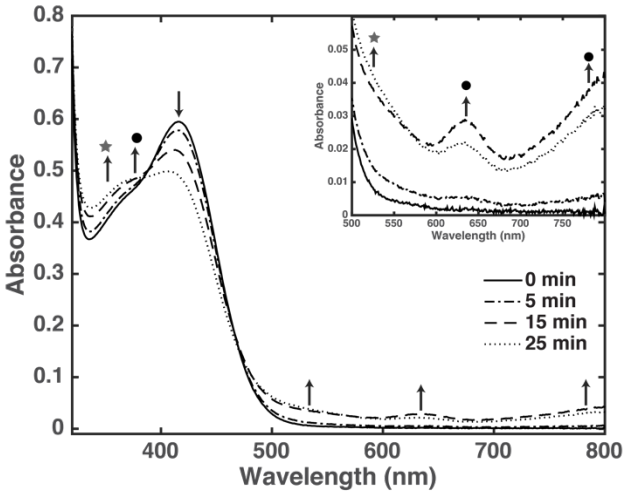

Figure S11 In situ UV-Vis spectral changes of **2** at -1.86 V vs Fc/Fc^{+} under Ar in 0.1 M TBAH in MeCN. The new peaks correspond to the formation of the following species: $[Mn(bpy)(CO)_3]^{-}$ (grey stars) and $[Mn_2(CO)_6(bpy)_2]$ (black circles). This is in agreement with the literature.[1,2]

References: (1) Bourrez, M.; Molton, F.; Chardon-Noblat, S.; Deronzier, A. *Angew. Chem. Int. Ed.* **2011**, *50* (42), 9903–9906. (2) Hartl, F.; Rossenaar, B. D.; Stor, G. J.; Stufkens, D. J. *Recl. Trav. Chim. Pays-Bas* **1995**, *114* (11–12), 565–570.

^{1}H NMR of 1

Temperature: 22 °C Solvent: Dichloromethane-d_2

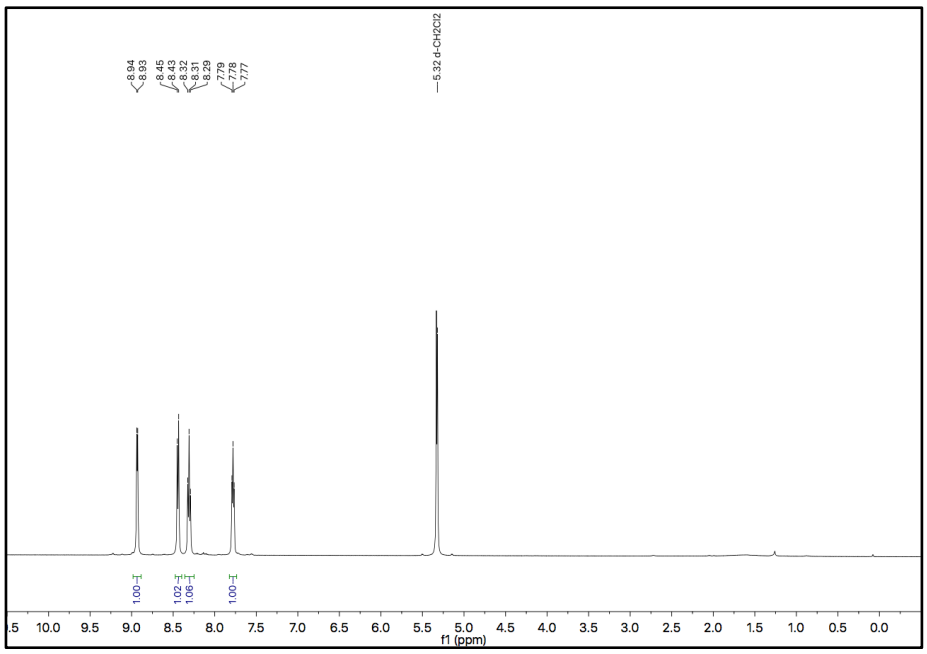

^{13}C NMR of 1

Temperature: 22 °C
Solvent: Dichloromethane-d_2

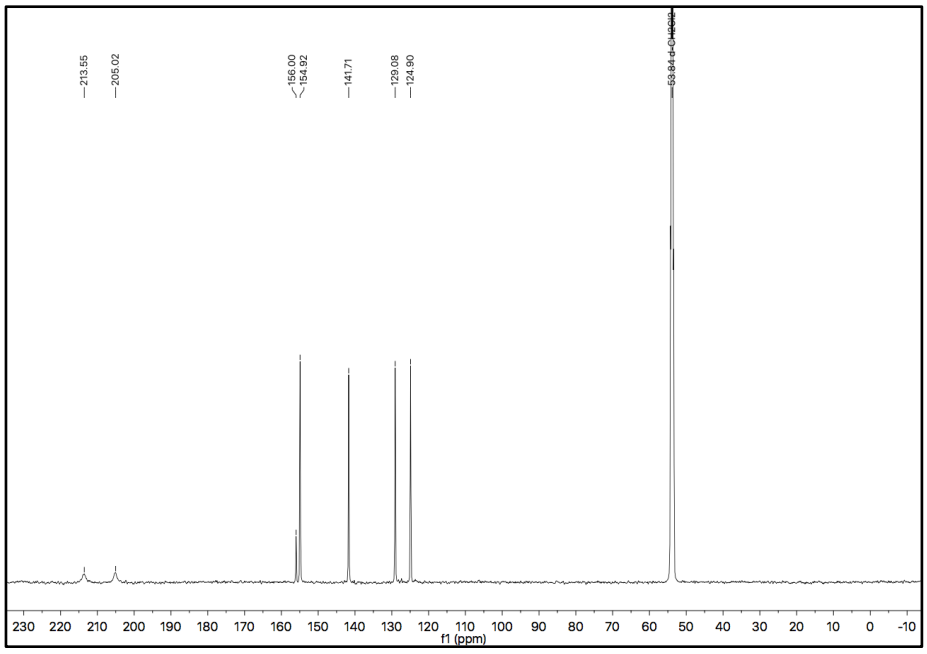

X-ray Crystallography

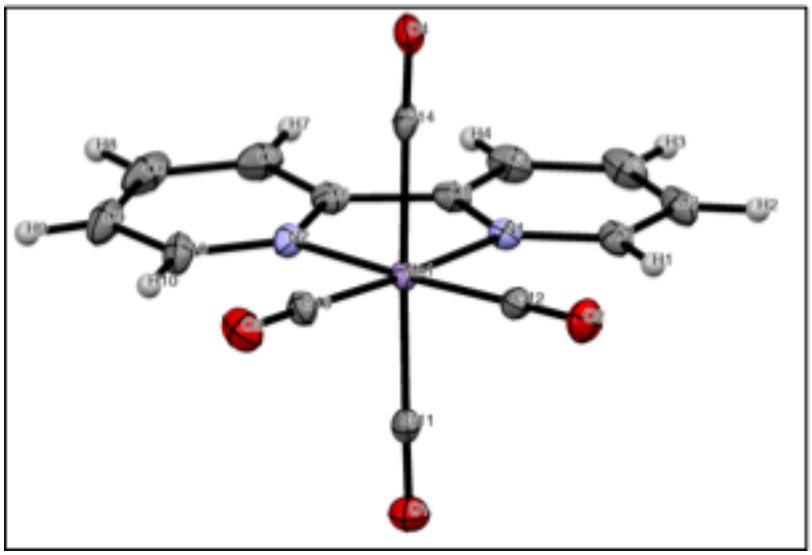

Collection Data for **1** Formula: $C_{15}H_{10}Cl_2F_6MnN_2O_4Sb$
Formula Weight: 643.85 g/mol
Crystal System: monoclinic
Space Group: P $2_1/n$
Unit Cell Dimensions:
a = 10.8094(7) Å alpha = 90°
b = 17.2883(10) Å beta = 92.010(2)°
c = 11.0181(7) Å gamma = 90°
Cell Volume: 2057.8(2) $Å^3$
Temperature: 100 K
Radiation Type: Mo Kα
Radiation Wavelength: 0.71073 Å
Theta range for data collection: 2.59° to 31.1°
Reflections Collected: 66616
Goodness-of-fit on F^2: 1.206
Bond Lengths (Å):

Sb1	F1	1.873(2)
Sb1	F2	1.883(2)
Sb1	F3	1.870(2)
Sb1	F4	1.878(2)
Sb1	F5	1.877(2)
Sb1	F6	1.861(2)
Mn1	N1	2.048(3)
Mn1	N2	2.044(3)
Mn1	C11	1.879(3)
Mn1	C12	1.825(3)
Mn1	C13	1.837(3)

Mn1	C14	1.915(3)
O1	C11	1.114(5)
N1	C1	1.340(5)
N1	C5	1.359(5)
C1	H1	0.95
C1	C2	1.392(5)
O2	C12	1.141(5)
N2	C6	1.360(5)
N2	C10	1.346(5)
C2	H2	0.951
C2	C3	1.378(5)
O3	C13	1.135(5)
C3	H3	0.95
C3	C4	1.382(6)
O4	C14	1.098(5)
C4	H4	0.95
C4	C5	1.385(5)
C5	C6	1.477(5)
C6	C7	1.388(5)
C7	H7	0.95
C7	C8	1.385(7)
C8	H8	0.951
C8	C9	1.382(6)
C9	H9	0.95
C9	C10	1.383(5)
C10	H10	0.95
Cl1	C15	1.760(5)
Cl2	C15	1.763(4)
C15	H15A	0.99
C15	H15B	0.99

Bond Angles (°):

F1	Sb1	F2	89.3(1)
F1	Sb1	F3	178.4(1)
F1	Sb1	F4	90.3(1)
F1	Sb1	F5	89.1(1)
F1	Sb1	F6	90.5(1)
F2	Sb1	F3	89.3(1)
F2	Sb1	F4	178.8(1)

F2	Sb1	F5	89.6(1)
F2	Sb1	F6	90.8(1)
F3	Sb1	F4	91.1(1)
F3	Sb1	F5	90.0(1)
F3	Sb1	F6	90.4(1)
F4	Sb1	F5	89.3(1)
F4	Sb1	F6	90.3(1)
F5	Sb1	F6	179.4(1)
N1	Mn1	N2	79.0(1)
N1	Mn1	C11	89.5(1)
N1	Mn1	C12	95.9(1)
N1	Mn1	C13	174.8(1)
N1	Mn1	C14	87.5(1)
N2	Mn1	C11	89.7(1)
N2	Mn1	C12	174.9(1)
N2	Mn1	C13	95.9(1)
N2	Mn1	C14	89.5(1)
C11	Mn1	C12	90.7(1)
C11	Mn1	C13	91.4(1)
C11	Mn1	C14	177.0(1)
C12	Mn1	C13	89.2(1)
C12	Mn1	C14	89.9(1)
C13	Mn1	C14	91.6(1)
Mn1	N1	C1	125.7(2)
Mn1	N1	C5	115.7(2)
C1	N1	C5	118.6(3)
N1	C1	H1	118.9
N1	C1	C2	122.3(3)
H1	C1	C2	118.8
Mn1	N2	C6	115.8(2)
Mn1	N2	C10	125.9(3)
C6	N2	C10	118.3(3)
C1	C2	H2	120.5
C1	C2	C3	118.9(3)
H2	C2	C3	120.6
C2	C3	H3	120.3
C2	C3	C4	119.4(4)
H3	C3	C4	120.3

C3	C4	H4	120.4
C3	C4	C5	119.2(4)
H4	C4	C5	120.5
N1	C5	C4	121.7(3)
N1	C5	C6	114.6(3)
C4	C5	C6	123.7(3)
N2	C6	C5	114.4(3)
N2	C6	C7	121.5(3)
C5	C6	C7	124.1(3)
C6	C7	H7	120.3
C6	C7	C8	119.5(4)
H7	C7	C8	120.2
C7	C8	H8	120.5
C7	C8	C9	118.8(4)
H8	C8	C9	120.7
C8	C9	H9	120.4
C8	C9	C10	119.2(4)
H9	C9	C10	120.4
N2	C10	C9	122.5(4)
N2	C10	H10	118.7
C9	C10	H10	118.8
Mn1	C11	O1	178.5(3)
Mn1	C12	O2	178.8(3)
Mn1	C13	O3	178.0(3)
Mn1	C14	O4	178.5(3)
Cl1	C15	Cl2	110.6(2)
Cl1	C15	H15A	109.6
Cl1	C15	H15B	109.5
Cl2	C15	H15A	109.5
Cl2	C15	H15B	109.5
H15A	C15	H15B	108.1